

High power N2 laser with a modified gas flow system and discharge geometry

Thomas Baby, T. Ramachandran, K. Sathianandan, V. P. N. Nampoori, and C. P. G. Vallabhan

Citation: *Rev. Sci. Instrum.* **62**, 2076 (1991); doi: 10.1063/1.1142369

View online: <http://dx.doi.org/10.1063/1.1142369>

View Table of Contents: <http://rsi.aip.org/resource/1/RSINAK/v62/i9>

Published by the [American Institute of Physics](#).

Related Articles

Determination of internal parameters for AlGaIn-cladding-free m-plane InGaIn/GaN laser diodes
Appl. Phys. Lett. **99**, 171115 (2011)

High-power blue-violet AlGaIn-cladding-free m-plane InGaIn/GaN laser diodes
Appl. Phys. Lett. **99**, 171113 (2011)

A single spectral mode wide stripe laser with very narrow linewidth
Appl. Phys. Lett. **99**, 171109 (2011)

Polarization dependent study of gain anisotropy in semipolar InGaIn lasers
Appl. Phys. Lett. **99**, 171105 (2011)

Photo-triggering and secondary electron produced ionization in electric discharge ArF* excimer lasers
J. Appl. Phys. **110**, 083304 (2011)

Additional information on *Rev. Sci. Instrum.*

Journal Homepage: <http://rsi.aip.org>

Journal Information: http://rsi.aip.org/about/about_the_journal

Top downloads: http://rsi.aip.org/features/most_downloaded

Information for Authors: <http://rsi.aip.org/authors>

ADVERTISEMENT

**AIP**Advances

Submit Now

**Explore AIP's new
open-access journal**

- **Article-level metrics
now available**
- **Join the conversation!
Rate & comment on articles**

High power N₂ laser with a modified gas flow system and discharge geometry

Thomas Baby,^{a)} T. Ramachandran, K. Sathianandan, V. P. N. Nampoori, and C. P. G. Vallabhan
Laser Division, Department of Physics, Cochin University of Science and Technology, Cochin-682 022, India

(Received 25 March 1991; accepted for publication 28 May 1991)

A high power N₂ laser of the double-Blumlein type having a modified gas flow system, electrode configuration, and discharge geometry with minimum inductance is described. By incorporating a triggered-pressurized spark gap switch, arc-free operation was achieved for a wide E/P range. The device gives a peak power in excess of 700 kW with a FWHM of 3 ns and an efficiency of 0.51%, which is remarkably high for a pulsed nitrogen laser system. The dependence of output power on parameters such as operating pressure, voltage, and repetition rate are discussed.

I. INTRODUCTION

The N₂ laser operating at 337.1 nm is a typical UV light source that can easily produce short optical pulses of high peak power and therefore has been used for a pumping source of dye lasers and photochemistry applications. Laser action in nitrogen at pressures of the order of 40 Torr was first observed by Heard,¹ which corresponds to the $V'=0 \rightarrow V''=0$ transition of the second positive system ($C^3\pi_u \rightarrow B^3\pi_g$). For a nitrogen laser, a smaller lifetime of the upper level (40 ns) compared to that of the lower laser level (10 μ s) calls for a design in which as many molecules as possible can be excited to the upper level within about 40 ns. Several designs for attaining high output power from N₂ lasers have been reported,²⁻⁵ but most of those lasers do not seem to be suitable for practical use because of the longer electrode, the high applied voltage, and the large value of the capacitance. We report some of the results obtained from our study of a low inductance pulsed N₂ laser that holds some promise in this direction.

We have fabricated a nitrogen laser of transverse discharge type similar to those described by Godard² and Basting, Schaffer, and Steyer;⁶ however, it differs in several important respects. The laser cavity and spark gap switch are designed in such a way that their physical sizes were kept minimum to lower the inductance. The salient features of the present design of the N₂ laser are (1) modified electrode configuration so as to give uniform and reproducible discharge; (2) tapered structure of the discharge tube suitable to produce stable laser pulses of short duration; (3) gas flow arrangement to obtain uniform pressure in the discharge tube; and (4) low inductance triggered-pressurized spark gap switch suitable for high current and fast discharge. Details of the design and fabrication of the pressurized spark gap switch and trigger circuit are described elsewhere.⁷ We observed significantly improved discharge uniformity and suppression of arcs over a wide pressure range; good reproducibility of both spatial distribution and intensity of the laser output; and increase in the range of

permissible operating pressures. Results obtained from the design analysis and parametric studies of the high efficiency N₂ laser is described in this article.

Pulsed N₂ laser emission at 337.1 nm requires large current densities (≈ 1 kA/cm²) and high electron temperature (≈ 5 eV). These values can be achieved by operating the laser with sufficiently high E/P , which can be obtained in a transverse discharge configuration. In the present work, the N₂ laser is typically operated with electric fields of 4.7–11.2 kV/cm and pressures at 10–200 Torr. Several authors^{8,9} have shown that the electron distribution function for a nitrogen discharge is closely approximated by a Maxwellian function when the electric field divided by the pressure exceeds about 30 to 90 V/cm Torr and the N₂ lasers efficiently lase at higher E/P values. In the present case, for the double-Blumlein circuit, the peak power is maximum when $E/P \sim 125$ V/cm Torr ($T_e = 5.20$ eV).

II. LASER DESIGN

The laser cavity is made of two rectangular aluminum bars (60 \times 5 \times 1.6) cm separated by 1.2-cm-thick perspex walls at the top and bottom. The two aluminum electrodes are 54 cm in effective length and form part of the cavity of the plasma tube so as to reduce the inductance.

Theoretical analysis had shown that in order to have the interelectrode gap uniformly filled with plasma, it is advisable to use a cylindrical cathode and plane anode.¹⁰ Hence, a combination of cylindrical cathode and plane anode has been used as electrodes to obtain uniform and reproducible discharge (Fig. 1). The cross-sectional view of the laser discharge channel is shown in Fig. 2. The separation between the electrodes is 11.2 mm at the rear side and 12.3 mm at the front side (output side). Presumably, the tapered structure of the discharge tube results in the electrical excitation occurring first at the mirror end and progressing towards the output end of the laser channel. This traveling wave excitation can result in comparatively short laser pulses. The optical cavity of the laser

^{a)}On leave from Rubber Research Institute of India, Kottayam-686 009, India.

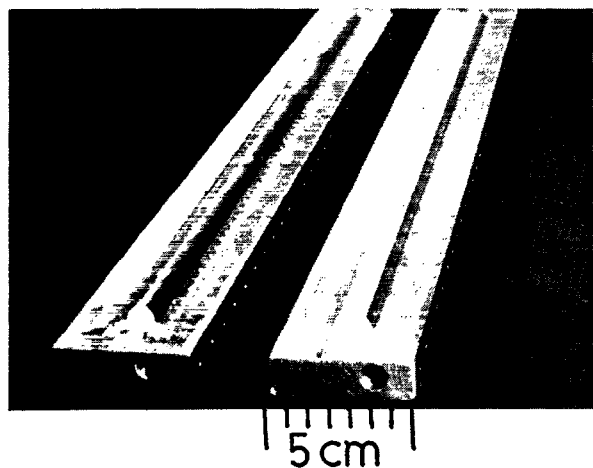


FIG. 1. Electrodes: cylindrical cathode and plane anode.

employs two windows that are mounted on the ends. A partially reflecting mirror of 80% reflectivity and a quartz window were used at the rear and the output end of the laser.

It is necessary that the residual ionization remaining due to the previous pulsed discharge should be distributed uniformly and with sufficient number density throughout the gas flow in order to seed the next discharge.¹¹ To achieve this aim, the aluminum bars are drilled axially to form the gas chamber of 0.5 cm diameter. In order to maintain a uniform gas flow, 60 holes of different diameters with 1 cm spacing are drilled on the inside surface of the electrodes (see Fig. 1) and these holes opens into the gas chamber. Sufficiently uniform gas flow can be achieved with these holes distributed along each electrode and located so that these holes are not opposite to each other.

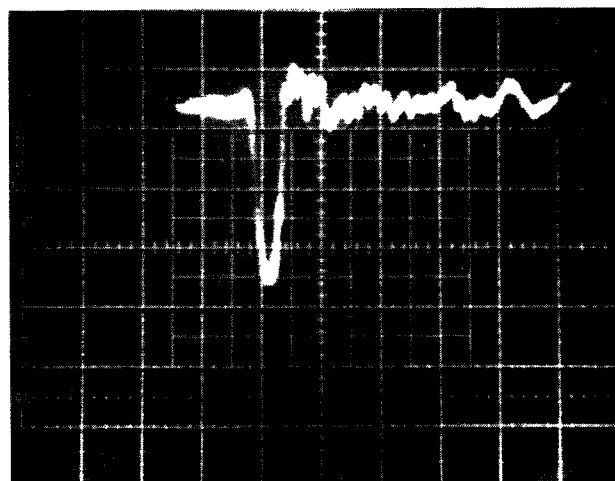


FIG. 3. Nitrogen laser pulse shape. Sweep speed: 5 ns/div and gain: 0.5 V/div.

Nitrogen gas is supplied through an inlet manifold fixed behind the electrode. The gas flows across the tube and is collected by an exhaust manifold in the other electrode.

The transmission line consists of double-sided copper clad fiberglass epoxy laminates (grade CFG 6/2DS, supplied by M/s. Formica India Ltd.) of dimensions 127×62 cm with thicknesses 1.6 mm which are charged to high voltage and can be discharged into the plasma tube via a triggered-pressurized spark gap switch.⁷ The size of the spark gap was kept minimal so as to limit its inductance to within a few nanoHenries. The low inductance of the fabricated spark gap helped to attain a high overvoltage across the laser electrodes. The pulse repetition frequency can be set between 0.1 Hz and 1 kHz. The double-sided copper clad epoxy sheet has a propagation delay time of 14.28 ns/m and can store sufficiently high electrical energy. For example, at 12 kV input voltage, the system can store an electrical energy ($CV^2/2$) of 1.15 J. The characteristic impedance Z was 0.26Ω and capacitance C was 15.98 nF.

III. RESULTS AND DISCUSSION

The average output power of the laser was measured using a Scientech model 38-0101 volume absorbing 1 in. disk calorimeter (thermopile) and displayed by a laser power meter (Scientech model 362). The energy per pulse was obtained by dividing the average power by repetition rate while the peak power was obtained by dividing the energy/pulse by the pulse width at FWHM. The overall efficiency was calculated by dividing the optical output energy per pulse by the stored electrical energy ($CV^2/2$). It was found that the laser gave an output energy/pulse of 0.21 mJ at 9.3 kV with a repetition rate of 8.8 Hz. The peak power output obtained was 700 kW (pressure: 90 Torr). The maximum conversion efficiency obtained was 0.51%, which is remarkably high for an N_2 laser compared to earlier reports.¹¹⁻¹⁵ The high power and conversion efficiency obtained using the present design is attributed to the low inductance of the system.

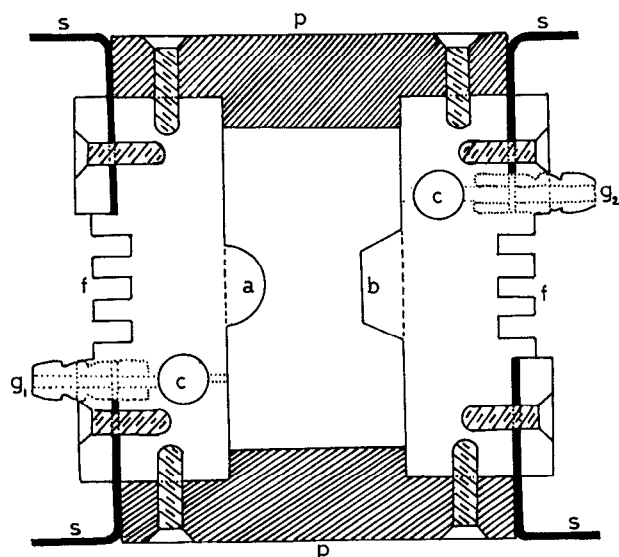


FIG. 2. Cross-sectional view of the laser discharge channel. *a*-cathode, *b*-anode, *c*-gas manifold, *g*₁ and *g*₂-gas inlet and outlet, *f*-cooling fin, *p*-perspex top and bottom, *s*-copper sheet as connecting leads.

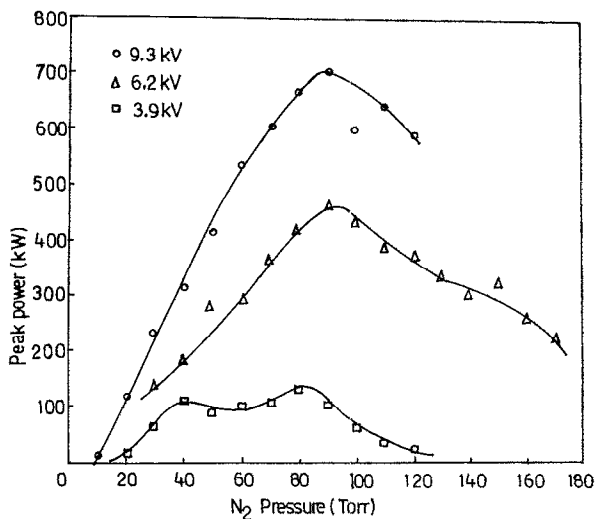


FIG. 4. Intensity variation of peak power with pressure for different voltages.

The output pulse shape recorded on a 466 DM44 Tektronix storage oscilloscope using a HP-2-4207 Hewlett Packard photodiode is shown in Fig. 3. The measured pulse width is 3 ns (FWHM). Since the propagation delay time of the storage line is smaller than that which is possible with the conventional designs, the laser gave slightly shorter duration pulses. The laser beam size is rectangular with dimensions of (1.7 × 0.8) cm outside the exit window. The horizontal divergence of the beam at half angle is 24 mrad while the vertical divergence is 3.5 mrad at half angle.

The variation of output peak power with pressure for different charging voltages shows that for a given voltage, the power increases, first reaching a maximum, and then decreases with further increase of pressure (Fig. 4) similar to the observations made by previous workers.

In practice, the peak applied voltage V_0 can be used for the calculation of the instantaneous electric field E by using the relation

$$E = \sqrt{2}V_0/d \text{ V/cm}, \quad (1)$$

where d is the electrode separation in cm. In the present design, the average value for $d = 1.18$ cm.

For nitrogen lasers with E/P in the range of 20 to 150 V/cm Torr, Fitzsimmons *et al.*¹¹ have shown that

$$KT_e = 0.11(E/P)^{0.80} \text{ eV}, \quad (2)$$

where T_e is the electron temperature.

Since the maximum laser output power of nitrogen laser occurs with E/P ratios in the range 60–125 V/cm Torr, the laser plasma can be described in terms of an electron temperature given by Eq. (2). The E/P values and electron temperatures (KT_e) for different pressures and voltages are tabulated in Table I. The initial increase in the laser power with increasing pressure is due to the fact that the number of molecules available for population inversion keeps on increasing with the pressure while the

TABLE I. Nitrogen laser discharge parameters.

Transmission line	Applied voltage V_0 (kV)	Electric field (E) (kV/cm)	Optimum pressure P (Torr)	Optimum E/P (V/cm Torr)	Electron temp. KT_e (eV)
Double-Blumlein circuit	3.9	4.7	80	58.7	2.9
	5.0	6.0	80	75.0	3.5
	6.2	7.4	90	82.6	3.8
	8.7	10.5	90	116.0	4.9
	9.3	11.2	90	124.7	5.2

electron temperature of the plasma remaining fairly high. At high N_2 pressures, the electron temperature T_e decreases due to collisional energy losses and hence both the rate of ionization and excitation fall, thereby reducing the output of the laser power due to onset of arcing, while at low pressures, although the electron temperature is high, the number of molecules available for laser action is small and hence the output power decreases.

The variation of output peak power with the applied voltage at corresponding optimum pressure shows a non-linearity in the graph (shown in Fig. 5), unlike the results reported by many of the authors^{2,6,16-19} except Ritcher, Kimel, and Moulton.²⁰ Following Ritcher and co-workers, the nonlinearity can be explained on the basis of the voltage dependence of electron temperature.

The output power is

$$W_p \propto \phi_+(l, t_p)\sigma(T_e)N_e. \quad (3)$$

Here N_e is the electron density, σ is the sum of the electron excitation cross section to the upper and lower laser levels, and $\phi_+(l, t_p)$ is the value of output peak photon density. The above equation shows that W_p increases linearly with N_e . It means that the output power increases as the voltage applied to the storage capacitor increases. The dependence

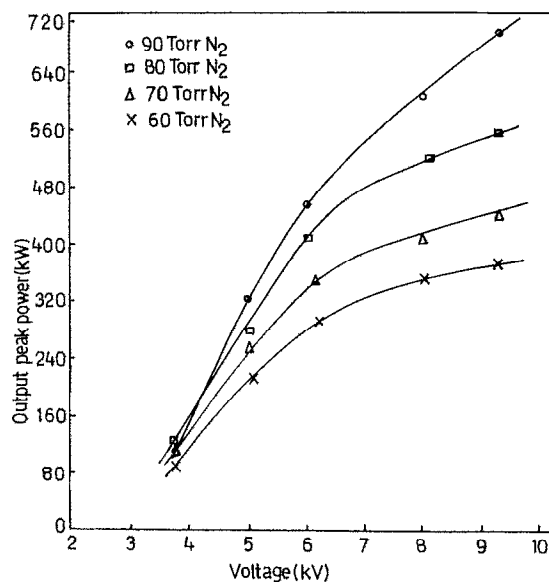


FIG. 5. Intensity variation of peak power with voltage for different pressures.

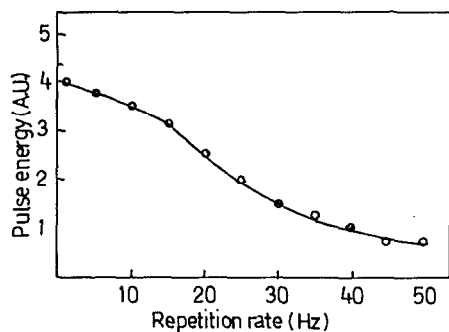


FIG. 6. Variation of pulse energy with repetition rate.

of T_e with voltage shows a saturation at higher discharge voltage. The deviation from nonlinearity originates from the voltage dependence of T_e and therefore also $\sigma(T_e)$, which in turn depends on the charging voltage.

The pulse energy is drastically reduced with an increase in the pulse repetition frequency (Fig. 6). This is due to the change in the initial preionization conditions prevailing in the plasma tube before each pulse. By increasing the time interval between two successive pulses (by decreasing the pulse repetition rate) the initial ion density (preionization) for each pulse is reduced. The lower the initial ion density, the higher will be the power of the laser beam.²¹

Figure 7 shows the dependence of efficiency on the applied voltage. The maximum efficiency obtained is 0.51% at a charging voltage of 6.2 kV. It may be noted that

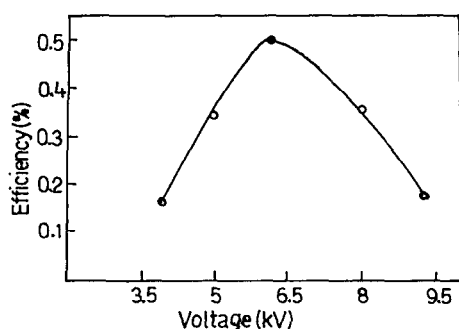


FIG. 7. Variation of maximum efficiency with voltage.

the highest efficiency (1%) reported so far for laser action in nitrogen is by Godard.²

In conclusion, a reliable Blumlein-driven nitrogen laser that has a modified gas flow system and discharge geometry has been developed. Peak power in excess of 700 kW with a FWHM of 3 ns and maximum efficiency of 0.51% was obtained. The laser described has been operating for several months in our laboratory giving satisfactory performance. The laser is being used to pump a dye laser system fabricated in our laboratory. The output power of the laser is more than sufficient to pump all of the commonly used visible wavelength laser dyes. The laser has been used for the study of fluorescence of impurity ions in single crystals and also for the study of decay times of this radiation. The low cost device utilizes only commonly available materials for its fabrication.

ACKNOWLEDGMENTS

The authors are thankful to Dr. T. M. A. Rasheed for many valuable discussions. They are also thankful to Professor K. Babu Joseph for providing them with necessary facilities to carry out this work.

- ¹ H. G. Heard, *Nature* **200**, 667 (1963).
- ² B. Godard, *IEEE J. Quantum Electron.* **QE-10**, 147 (1974).
- ³ E. Armandillo and A. J. Kearsley, *Appl. Phys. Lett.* **47**, 611 (1982).
- ⁴ H. ds. Reis, A. D. Tavares, Jr., C. A. Massone, and M. S. Z. Chahat, *J. Phys. E* **19**, 471 (1986).
- ⁵ Y. Saito, A. Nomura, and T. Kano, *Rev. Sci. Instrum.* **58**, 162 (1987).
- ⁶ D. Basting, F. P. Schaffer, and B. Steyer, *Opto-electron.* **4**, 43 (1972).
- ⁷ T. Baby, T. Ramachandran, P. Radhakrishnan, V. P. N. Nampoori, and C. P. G. Vallabhan, *J. Phys. E* (in press).
- ⁸ A. G. Englhardt, A. V. Phelps, and C. G. Risk, *Phys. Rev.* **135**, 1566 (1964).
- ⁹ L. E. Kline and J. G. Siambis, *Phys. Rev. A* **5**, 794 (1972).
- ¹⁰ A. V. Armichev, V. S. Aleinikov and T. B. Fogelson, *Sov. J. Quantum Electron.* **10**, 592 (1982).
- ¹¹ W. A. Fitzsimmons, L. W. Anderson, C. E. Reidhauser, and Jan. M. Vritilet, *J. Quantum Electron.* **QE-12**, 624 (1976).
- ¹² I. Baltog, M. Ganciu, L. Mihut, and V. Zambreanu, *J. Phys. E* **19**, 1030 (1986).
- ¹³ B. S. Patel, *Rev. Sci. Instrum.* **49**, 1361 (1978).
- ¹⁴ E. E. Bergmann, *Appl. Phys. Lett.* **28**, 84 (1976).
- ¹⁵ K. H. Krahn, *J. Appl. Phys.* **50**, 6656 (1979).
- ¹⁶ M. Geller, D. E. Altman, and T. A. De. Temple, *Appl. Opt.* **7**, 2232 (1968).
- ¹⁷ S. C. Mehendale and D. D. Bhawalkar, *J. Appl. Phys.* **53**, 6444 (1982).
- ¹⁸ E. E. Bergmann, *Appl. Phys. Lett.* **31**, 661 (1977).
- ¹⁹ J. P. Singh and S. N. Thakur, *J. Sci. Ind. Res.* **23**, 227 (1978).
- ²⁰ P. Richter, J. D. Kimel, and G. C. Moulton, *Appl. Opt.* **15**, 756 (1976).
- ²¹ A. Persephonis, *Opt. Commun.* **62**, 265 (1987).